Molecular Microbiology (2009) 71(5), 1071–1087
doi:10.1111/j.1365-2958.2008.06572.x
First published online 3 February 2009

Bacterial toxin YafQ is an endoribonuclease that associates with the ribosome and blocks translation elongation through sequence-specific and frame-dependent mRNA cleavage

Meredith H. Prysak,[1†] Christopher J. Mozdzierz,[1†] Angela M. Cook,[1] Ling Zhu,[2] Yonglong Zhang,[2] Masayori Inouye[2] and Nancy A. Woychik[1*]
Departments of [1]Molecular Genetics, Microbiology and Immunology, [2]Biochemistry, UMDNJ-Robert Wood Johnson Medical School, 675 Hoes Lane, Piscataway, NJ 08854, USA.

Summary

Toxin–antitoxin (TA) systems on the chromosomes of free-living bacteria appear to facilitate cell survival during intervals of stress by inducing a state of reversible growth arrest. However, upon prolonged stress, TA toxin action leads to cell death. They have been implicated in several clinically important phenomena – bacterial persistence during antibiotic treatment, biofilm formation and bacterial pathogenesis – and serve as attractive new antibiotic targets for pathogens. We determined the mode of action of the YafQ toxin of the DinJ–YafQ TA system. YafQ expression resulted in inhibition of translation, but not transcription or replication. Purified YafQ exhibited robust ribonuclease activity *in vitro* that was specifically blocked by the addition of DinJ. However, YafQ associated with ribosomes *in vivo* and facilitated rapid mRNA degradation near the 5′ end via cleavage at AAA lysine codons followed by a G or A. YafQ(H87Q) mutants lost toxicity and cleavage activity but retained ribosome association. Finally, LexA bound to the *dinJ–yafQ* palindrome and triggered module transcription after DNA damage. YafQ function is distinct from other TA toxins: it associates with the ribosome through the 50S subunit and mediates sequence-specific and frame-dependent mRNA cleavage at $^{5'}$AAA – G/A$^{3'}$ sequences leading to rapid decay possibly facilitated by the mRNA degradosome.

Accepted 3 December, 2008. *For correspondence. E-mail nancy.woychik@umdnj.edu; Tel. (+1) 732 235 4534; Fax (+1) 732 235 5223. †These two authors contributed equally to this work.

Introduction

Toxin–antitoxin (TA) systems/modules (also referred to as addiction or suicide modules) were first identified on plasmids due to their ability to induce post-segregational killing, because the cell becomes dependent on the presence of the TA-harbouring plasmid for survival (Gerdes *et al.*, 1986). However, these TA systems are also present on the chromosomes of free-living bacteria. Chromosomal TA modules typically comprise an autoregulated operon minimally encoding both a labile antitoxin and a more stable toxic protein (Gerdes *et al.*, 2005). All characterized chromosomal TA toxins facilitate inhibition of cell growth by targeting essential cell processes such as replication and translation. This inhibition appears to be an adaptation that facilitates stress survival. TA toxin-mediated growth arrest is reversible up to a 'point of no return', beyond which cell death occurs (Pedersen *et al.*, 2002). The function of the antitoxin, in contrast, is to prevent toxin activity during normal growth and enable finely tuned control of TA module toxicity during relatively short periods of environmental stress (Gerdes *et al.*, 2005).

There are five confirmed chromosomal TA loci in *Escherichia coli* K-12 cells: *relBE*, *yefM–yoeB*, *mazEF*, *chpBI-BK* and *hipBA* (Gerdes *et al.*, 2005). The toxins MazF and ChpBK are sequence-specific endoribonucleases that target free mRNA (independent of the ribosome) for degradation, thus indirectly perturbing translation (Christensen *et al.*, 2003; Zhang *et al.*, 2003; 2005a,b; Munoz-Gomez *et al.*, 2004). The RelE toxin also perturbs translation, but does so through interaction with the ribosome by preferentially targeting stop codons in a sequence-specific manner, with a preference for UAG (Christensen and Gerdes, 2003; Christensen *et al.*, 2001; Pedersen *et al.*, 2003). Although the *hipBA* TA system is poorly understood and its mechanism of toxicity is unknown, it appears to be a kinase whose action contributes to the formation of bacterial persisters upon antibiotic treatment (Keren *et al.*, 2004; Correia *et al.*, 2006; Korch and Hill, 2006). A sixth TA locus, *dinJ–yafQ*, has been recently identified (Motiejunaite *et al.*, 2007). The intracellular targets and precise mechanism of toxicity of YoeB, HipA and YafQ have not been identified.

In the present work, we characterized the basic properties of the DinJ–YafQ TA module and determined the mechanism of YafQ-mediated toxicity. YafQ expression resulted in translation, but not transcription or replication defects. Northern analysis revealed that mRNA was rapidly degraded in most, but not all, mRNAs tested following YafQ expression *in vivo*. Recombinant YafQ possessed robust ribonuclease activity *in vitro* that was blocked by addition of DinJ. Some degree of sequence specificity was detectable upon YafQ titration *in vitro*. However, YafQ associated with the 50S ribosomal subunit of the 70S ribosome *in vivo* and exhibited clear sequence-specific and frame-dependent endoribonuclease activity. Therefore, YafQ toxicity is distinct from other TA toxins: it associates with ribosomes, mediates mRNA cleavage at $^{5'}$AAA – G/A$^{3'}$ consensus sequences (which are well represented in mRNAs, especially at codon +2), leading to translation complex arrest shortly after the transition from the initiation to the elongation step.

Results

The DinJ–YafQ TA system

YafQ exhibits sequence similarity to the RelE family of TA toxins but remains largely uncharacterized (Gerdes *et al.*, 2005). YafQ has recently been identified as a possible toxin of a chromosomally encoded *E. coli* TA module based on its sequence similarity to two other such toxins, *relE* and *yoeB* (Gerdes *et al.*, 2005; Motiejunaite *et al.*, 2007). In addition, the gene immediately 5′ of *yafQ, dinJ*, shares sequence similarity to the *relB* and *yefM* antitoxins. The *dinJ–yafQ* module exhibits other features typical of a TA system: the genes are adjacent with minimal overlap/ *inJ–yafQ* are separated by tw encode small proteins (DinJ is 86 amino acids and 9.4 kDa; YafQ is 96 amino acids and 10.8 kDa), the proteins often have opposing isoelectric points (DinJ pI is 5.24, YafQ pI is 9.52) and a palindrome sequence is upstream of the module for transcriptional autoregulation (*dinJ–yafQ* has a palindrome containing a LexA box whose function is addressed later).

YIIIIKES! YafQ is 92 aa! Good grief.

In order to demonstrate that *yafQ* indeed encodes a toxic protein, we cloned *yafQ* onto the arabinose-inducible pBAD33 promoter. YafQ induction of mid-logarithmic *E. coli* cells resulted in complete and stable growth inhibition after 30 min (Fig. 1A). Plating of colony forming units was consistent with the growth profile (Fig. S1). Using the same strategy, DinJ overexpression did not result in any reduction in growth rate compared with wild-type cells (data not shown). However, coexpression of both antitoxin and toxin genes from the *dinJ–yafQ* module (Fig. 1B) or coinduction of *dinJ* and *yafQ* from independent plasmids (data not shown) resulted in normal growth. Therefore, DinJ is the cognate antitoxin of YafQ.

All proteic TA modules previously described are capable of forming a stable protein complex (Gerdes *et al.*, 2005). To test whether this is true of DinJ–YafQ, we expressed the *dinJ–yafQ* module from a pET plasmid that added a $(His)_6$ tag to the carboxy terminus of YafQ. The resulting cell extract was passed over a Ni-NTA column and both untagged DinJ and YafQ$(His)_6$ were recovered, demonstrating that DinJ and YafQ form a stable protein complex *in vivo* (Fig. 1C).

Another key feature of the physiological activity of TA systems is the relative instability of the antitoxins compared with their cognate toxins. In fact, several TA antitoxins have been demonstrated to be more susceptible to degradation by proteases Lon, ClpAP or ClpXP compared with their toxin counterparts (Gerdes *et al.*, 2005). Therefore, we tested if DinJ could be degraded by one of these three proteases *in vivo*. We expressed *dinJ* from an IPTG-inducible plasmid and followed DinJ protein levels by Western analysis after translation was blocked with hygromycin B in wild-type, Δ*lon*, Δ*clpP*, Δ*clpA* and Δ*clpX* strains (Fig. 1D). DinJ was substantially stabilized in Δ*lon*, Δ*clpP* and Δ*clpX* strains, but not the wild-type control and Δ*clpA* strain, suggesting that both ClpXP and Lon proteases play a dual role in the degradation of DinJ. Notably, several proteins that are highly induced and rapidly degraded after DNA damage are the targets of multiple proteases (Neher *et al.*, 2006). In fact, LexA is also cleaved by both Lon and ClpXP. In summary, our data demonstrated that *dinJ–yafQ* exhibits properties characteristic of TA systems.

YafQ expression inhibits translation

We next sought to identify which, if any, global cellular process might be perturbed in response to YafQ expression. We first used permeabilized *E. coli* cells as an *in vitro* approach to determine if toxin expression affects replication, transcription or translation by quantifying incorporation of isotope labelled precursors of DNA ([α-^{32}P]-dTTP), RNA ([α-^{32}P]-UTP) or protein ([^{35}S]-methionine) respectively. We harvested *E. coli* cells that had been grown with or without arabinose for YafQ induction, permeabilized their membranes after a brief exposure to toluene (Halegoua *et al.*, 1976a) and measured ATP-dependent DNA, RNA or protein synthesis (ATP must be supplied to drive energy requiring metabolic processes in permeabilized cells). We observed no differences in incorporation of [α-^{32}P]-dTTP and [α-^{32}P]-UTP in the YafQ-induced and uninduced cells (data not shown) consistent with published *in vivo* incorporation data (Motiejunaite *et al.*, 2007). However, a sustained drop in [^{35}S]-methionine incorporation into toluene-treated cells

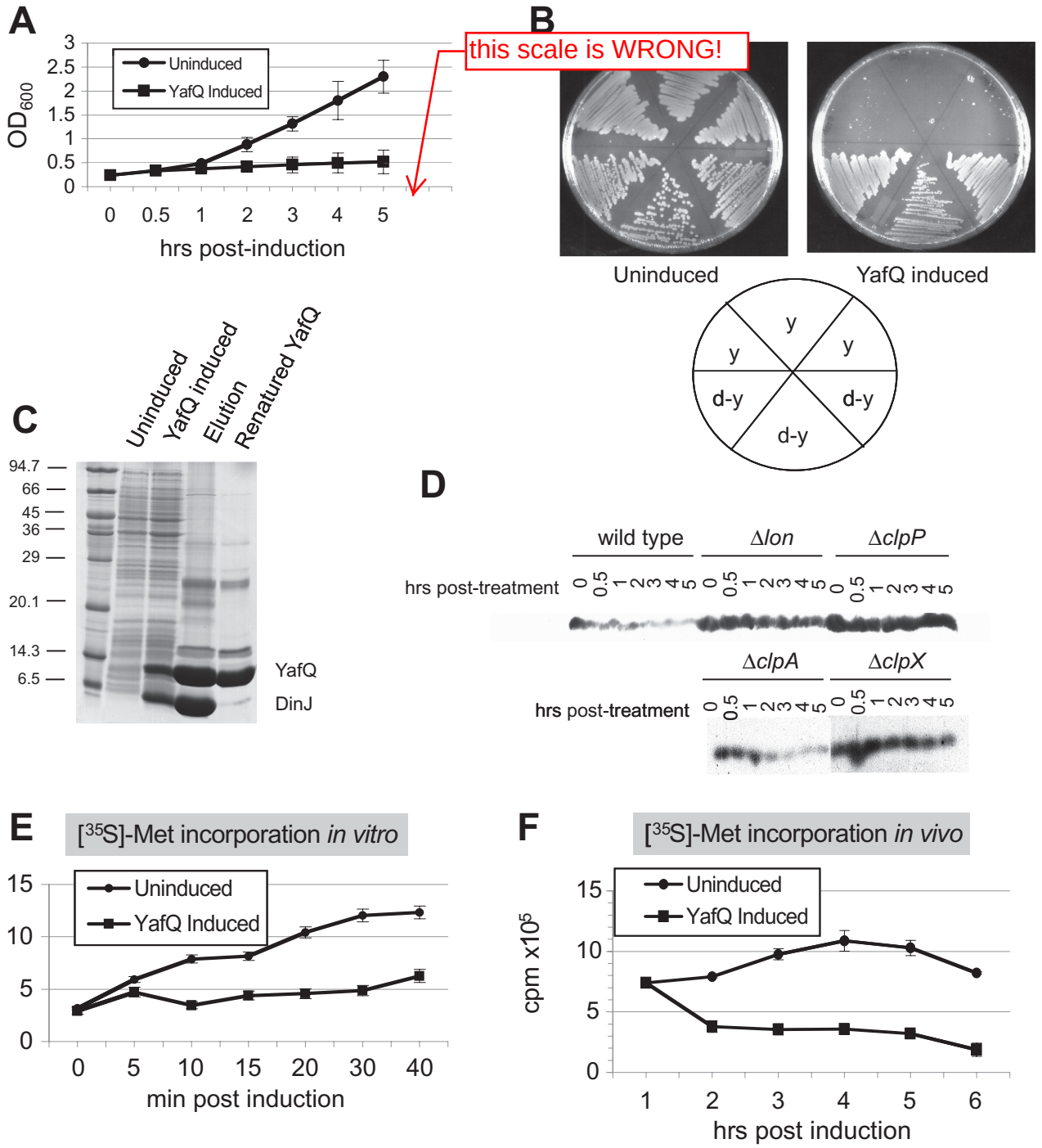

Fig. 1. Features of the DinJ–YafQ TA system.
A. YafQ expression leads to growth arrest. Growth profile of BW25113 cells containing pBAD33-YafQ grown at 37°C in LB-chloramphenicol with (induced) or without (uninduced) 0.2% arabinose; standard deviations result from two independent experiments.
B. DinJ can rescue YafQ-mediated growth arrest. Coexpression of the *dinJ–yafQ* module (d–y, bottom), *yafQ* alone (y, top) in pBAD33 on LB-chloramphenicol plates incubated at 37°C overnight with or without 0.2% arabinose.
C. DinJ copurifies with YafQ. BL21(DE3) [*dinJ-yaf*(*His*)$_6$-pET21c] cell lysate (induced) before Ni-NTA affinity chromatography to isolate the DinJ–YafQ(His)$_6$ complex (elution) and YafQ (renatured YafQ). Uninduced lane is the –IPTG control lysate. Molecular weight markers on the left.
D. DinJ is cleaved by Lon and ClpXP proteases. *BW25113* or isogenic protease deletion cells carrying *dinJ*-pINIII were IPTG induced before treatment with hygromycin B. Cell lysates were subjected to SDS-PAGE and Western analysis (using a polyclonal antibody to DinJ + YafQ) to determine DinJ stability.
E and F. YafQ inhibits translation *in vitro* and *in vivo*. Quantification of [^{35}S]-methionine incorporation in toluene treated (E) or living cells (F) with or without YafQ induction. Standard deviations in E and F result from two independent experiments.

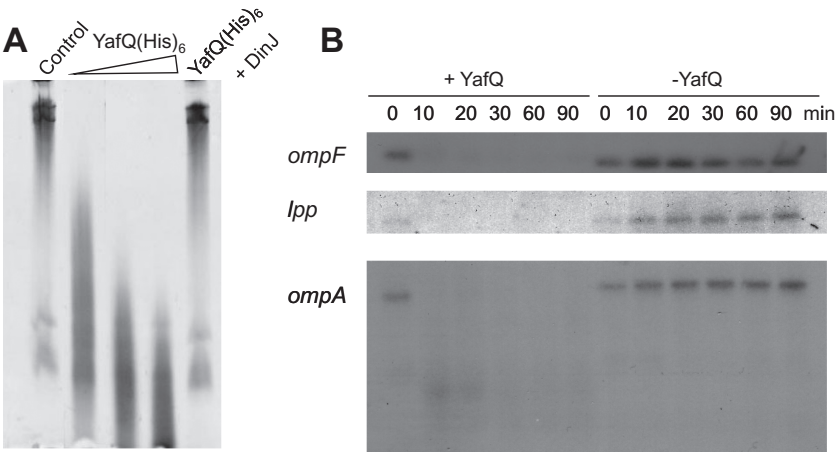

Fig. 2. YafQ targets mRNA *in vitro* and *in vivo*.
A. YafQ is a ribonuclease whose activity is blocked by DinJ. Control lane, 10 μg total RNA only. Increasing amounts (0.15, 0.3 and 0.6 μg respectively) of purified YafQ(His)$_6$ were added to 10 μg of total RNA (lanes 2–4). The YafQ(His)$_6$ + DinJ lane contained 0.6 μg of YafQ(His)$_6$ pre-incubated with 0.6 μg DinJ before addition to the RNA. RNA was separated on a 3% PAGE gel and visualized by EtBr.
B. YafQ expression leads to rapid loss of *ompA*, *ompF* and *lpp* mRNAs *in vivo*.

occurred shortly after YafQ induction, suggesting that YafQ expression blocks translation (Fig. 1E), consistent with earlier results of Motiejunaite *et al.* (2007).

Defects in translation are characterized by a severe and immediate reduction in [^{35}S]-methionine incorporation whereas RNA synthesis should not be significantly affected and DNA replication should not be affected until later time points (when labile, essential replication proteins cannot be replenished). We then measured *in vivo* [^{35}S]-methionine incorporation in YafQ-induced *E. coli* cells (Fig. 1F). Relative to the control, protein synthesis decreased by 50% after 30 min and by approximately 70% after 90 min. We also measured *in vivo* incorporation of radioactively labelled precursors of mRNA and DNA respectively, and obtained incorporation profiles consistent with defective translation (Fig. S2). Collectively, YafQ expression specifically disrupted *de novo* protein synthesis *in vivo*. A translational defect in response to expression is in keeping with the phenotype observed for many of the described chromosomally encoded *E. coli* TA modules, including RelE, a YafQ family member (Christensen *et al.*, 2001; 2004).

YafQ exhibits ribonuclease activity in vitro *and* in vivo

As chromosomal TA toxins MazF and ChpBK block translation through site-specific cleavage of mRNA independent of ribosomes (Zhang *et al.*, 2003; 2005b), we determined if YafQ possessed ribonuclease activity. We first assayed the activity of YafQ on RNA *in vitro*. Active YafQ(His)$_6$ was isolated from DinJ through a series of denaturation/renaturation steps and increasing amounts of recombinant toxin were added to a fixed amount of *E. coli* total RNA (Fig. 2A). We observed dose-dependent cleavage of total RNA by YafQ(His)$_6$. This cleavage was specifically due to the activity of YafQ(His)$_6$ and not a contaminating ribonuclease because the pre-incubation of YafQ(His)$_6$ with pure DinJ antitoxin before addition of RNA completely inhibited RNA cleavage (Fig. 2A). This finding is consistent with our previous data demonstrating that DinJ physically interacts with YafQ (Fig. 1C) and coexpression of DinJ with YafQ rescues the toxicity observed with YafQ expression alone (Fig. 1B).

We next examined steady-state levels of three highly expressed mRNAs (*ompA, ompF* and *lpp* encoding outer membrane protein A, outer membrane porin 1a and murein lipoprotein respectively) before, and at intervals after, YafQ induction in *E. coli* cells (Fig. 2B). We observed a rapid and complete or nearly complete loss of each of the three mRNAs upon YafQ expression. The steady-state levels of the respective control mRNAs without YafQ induction were either stable or increased with time. These data indicated that YafQ also mediates mRNA degradation *in vivo*.

Finally, we examined YafQ cleavage specificity *in vitro* with a recently developed assay (Zhu *et al.*, 2006) that utilizes a long, single-stranded RNA substrate (bacteriophage MS2 RNA). MS2 RNA is commercially available and comprises a nearly equal base content (26% G, 23% A, 26% C and 25% U) within its 3569 nucleotides. MS2, as with any long single-stranded RNA, tends to form extensive secondary structures. Therefore, the major cold shock protein and RNA chaperone that prevents secondary structure formation, CspA, was added to the reaction at a concentration known to saturate mRNA.

After careful titration of the same YafQ preparation used in Fig. 2A, we were able to clearly identify six specific cleavage sites upon primer extension analysis with selected MS2 oligonucleotides (Fig. 3). Notably, all six cleavage sites that we identified were YafQ-specific because cleavage activity was abrogated in the presence of the cognate DinJ antitoxin. The only apparent consensus sequence among the six cleavage sites was a GG doublet on either side of the cut site in five of the six sites (Fig. 3F). Unlike studies with the MazF toxin in this same assay, it was necessary to dilute the enzyme more

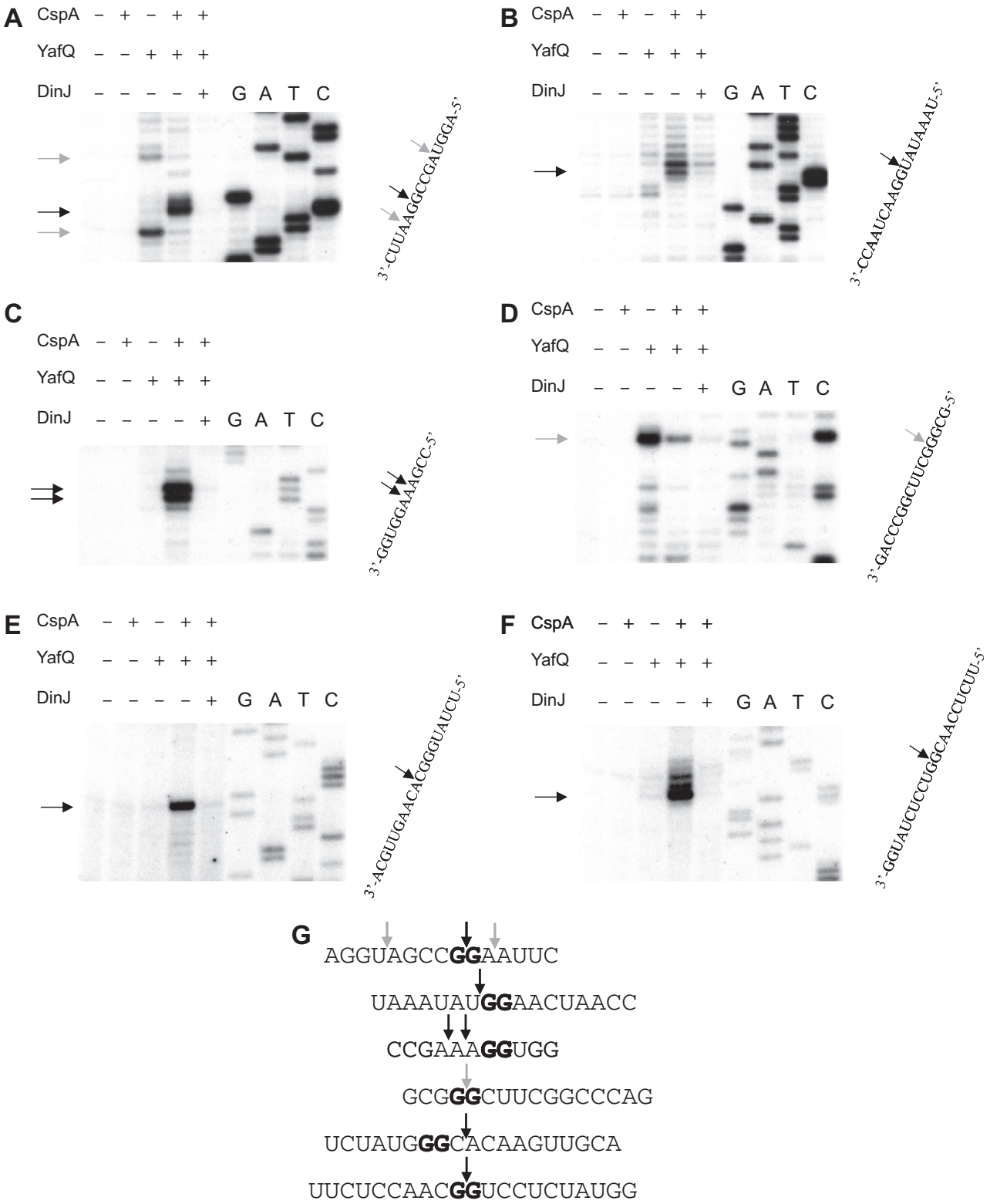

Fig. 3. YafQ site specificity *in vitro*.
A–F. Primer extension experiments after cleavage of MS2 RNA with YafQ(His)$_6$. Cleavage site either becomes visible or greatly enhanced by the addition of CspA to open up MS2 RNA secondary structure. Major cuts sites represented by black arrows, minor by grey arrows. The RNA recognition sequence is shown to the right and was derived from the RNA complement of the DNA sequencing ladder on the right. The same oligonucleotide was used for both the primer extension and sequencing reaction.
G. Alignment of sequences containing the YafQ cleavage site; the GG consensus is in bold.

Fig. 4. YafQ mediates sequence-specific and frame-dependent mRNA cleavage.
A. Primer extension analysis of the same mRNAs analysed in Fig. 2B, 90 min wild-type (wt) samples corresponding DNA sequences to the left. Primers were selected to show all major cleavage products on a single gel; FL, full-length products; exact cleavage positions of mRNAs near the top of the gel were determined with closer primers. YafQ consensus cleavage sites as indicated to the right. Putative RNase E sites shown in parentheses. The *ompF* 30 min lane was not loaded onto this gel but the products are similar to the time points before and after it. The sequencing ladder next to the lower *lpp* consensus does show a C band (G for the mRNA) in darker exposures; the sequence of the *ompF* ladder has a point mutation near the putative RNase E sequence; however, the correct sequence is typed to the right.
B. Summary of YafQ cleavage sites from panel A. Grey bars represent mRNAs (drawn to scale) of the coding region only (5′ and 3′ non-coding regions are absent). Only the first ~150 nucleotides of the 1089-nucleotide *ompF* coding region were analysed, shown in grey.
C. Alignment of the six major YafQ cleavage sites and the resulting consensus.

extensively because higher enzyme/substrate ratios [comparable to those used for MazF studies (Zhu *et al*., 2006)] resulted in comprehensive, non-specific cleavage; this observation was also consistent with the potent cleavage of RNAs exhibited by YafQ in Fig. 2A.

YafQ cleaves mRNAs at AAA (lysine) codons

Because YafQ exhibited potent ribonuclease activity *in vitro* and *in vivo*, we next tested whether YafQ exhibited sequence-specific endoribonuclease activity – a characteristic of the MazF and ChpBK TA toxins – by performing primer extension experiments with RNA prepared from YafQ induced cells. We expressed YafQ in an *E. coli* strain ('Δ6') that lacks the loci for each of the six known chromosomal TA modules (*mazEF*, *relBE*, *chpB*, *hipBA*, *yefM-yoeB* and *dinJ–yafQ*). Use of the Δ6 strain precluded mRNA cleavage as a consequence of downstream activation of other TA toxins resulting from the stress imparted by YafQ expression. We isolated total RNA from YafQ-induced and uninduced Δ6 cells and performed primer extension analyses on the same three transcripts subjected to Northern analysis, initially with primers ~150 nucleotides downstream of the 5′ end of the translation start site. We then performed additional primer extension experiments to enable nearly complete coverage of two mRNAs, *lpp* (237 base pairs) and *ompA (*1041 base pairs), allowing us to determine if YafQ-mediated cleavage was detectable elsewhere in the transcript. In total, we detected two YafQ-specific major cleavage sites for each mRNA (six total, Fig. 4A) revealing a minimal consensus recognition sequence of $^{5'}$AAA – G/A$^{3'}$ in which the AAA, encoding lysine, *must be in* frame (Fig. 4C); no cleavage was observed at either $^{5'}$XAA – A(G/A)X$^{3'}$ or $^{5'}$XXA – AA(G/A)$^{3'}$ sequences present in each the three mRNAs we tested (Fig. 4B).

Curiously, a non-consensus YafQ-dependent cleavage site was detected just downstream of the two major YafQ $^{5'}$AAA – G/A$^{3'}$ consensus cut sites in *ompF* (Fig. 4A). The AU-rich sequence of this cleavage site, $^{5'}$GCA$^{\downarrow}$UUAUU UUU$^{3'}$, matched the consensus for RNase E (Ehretsmann *et al*., 1992; Redko *et al*., 2003). RNase E is single-strand specific endoribonuclease required for rapid mRNA decay and accurate RNA processing in *E. coli*. Therefore, cleavage of *ompF* at $^{5'}$GCA$^{\downarrow}$UUAUUUUU3′ was likely the result of RNase E-mediated hydrolysis of a *ompF* fragments with free 5′ ends (either 5′ hydroxyl or 5′ monophosphate, depending on the mechanism of YafQ cleavage) that were generated upon YafQ cleavage. RNase E-mediated decay of YafQ-cleaved mRNA is consistent with the rapid decrease in steady-state mRNA levels noted for *ompF* (Fig. 2B). In fact, the rapid degradation of the *lpp* and *ompA* mRNAs also likely enlists the action of cellular RNases that cleave RNA fragments having free 5′ ends (Carpousis, 2007) generated upon YafQ hydrolysis *in vivo*. We detected another potential RNase E consensus site $^{5'}$UGG$^{\downarrow}$UUU3′ in *ompA* mRNA that precedes a ladder of light bands in the bottom third of the *ompA* primer extension panel; the ladder may represent products of 3′-5′ exoribonuclease(s), which are also major players in mRNA degradation (Fig. 4A). Likewise, darker exposures of the *lpp* primer extensions revealed the presence of several light bands after the initial strong cleavage by YafQ.

We noted several trends upon analysis of our primer extension data. First, the apparent consensus for ribosome-associated YafQ cleavage was an in-frame AAA lysine codon followed by a purine residue, $^{5'}$AAA – G/A$^{3'}$ (Fig. 4C); out of frame consensus sequences were well represented yet not cleaved (Fig. 4B). Second, of the three transcripts we tested, there was a preference for guanine at the fourth position (five of the six sites detected had G at position 4). Third, each of the six $^{5'}$AAA – G/A$^{3'}$ consensus sites identified were cut on the 5′ side of the third A of the AAA triplet (at the phosphodiester bond between the second and third adenine, i.e. $^{5'}$AA$^{\downarrow}$A–G/A$^{3'}$). Fourth, major cleavage sites were only found within 180 nucleotides of the translation start site even for large transcripts such as *ompA*, despite the presence of additional downstream consensus sequences. In fact, the second (and last) major cleavage site we detected for *ompA* was at codon 24 even though this mRNA comprises 347 codons with seven YafQ consensus sites after codon 24 (Fig. 4B), indicating a preference for cleavage early in the mRNA. Fifth, after YafQ cleavage, the RNA degradosome (Carpousis, 2007) appears to be enlisted to facilitate a secondary mechanism driving the rapid, complete degradation of mRNAs. Sixth, the first major YafQ cleav-

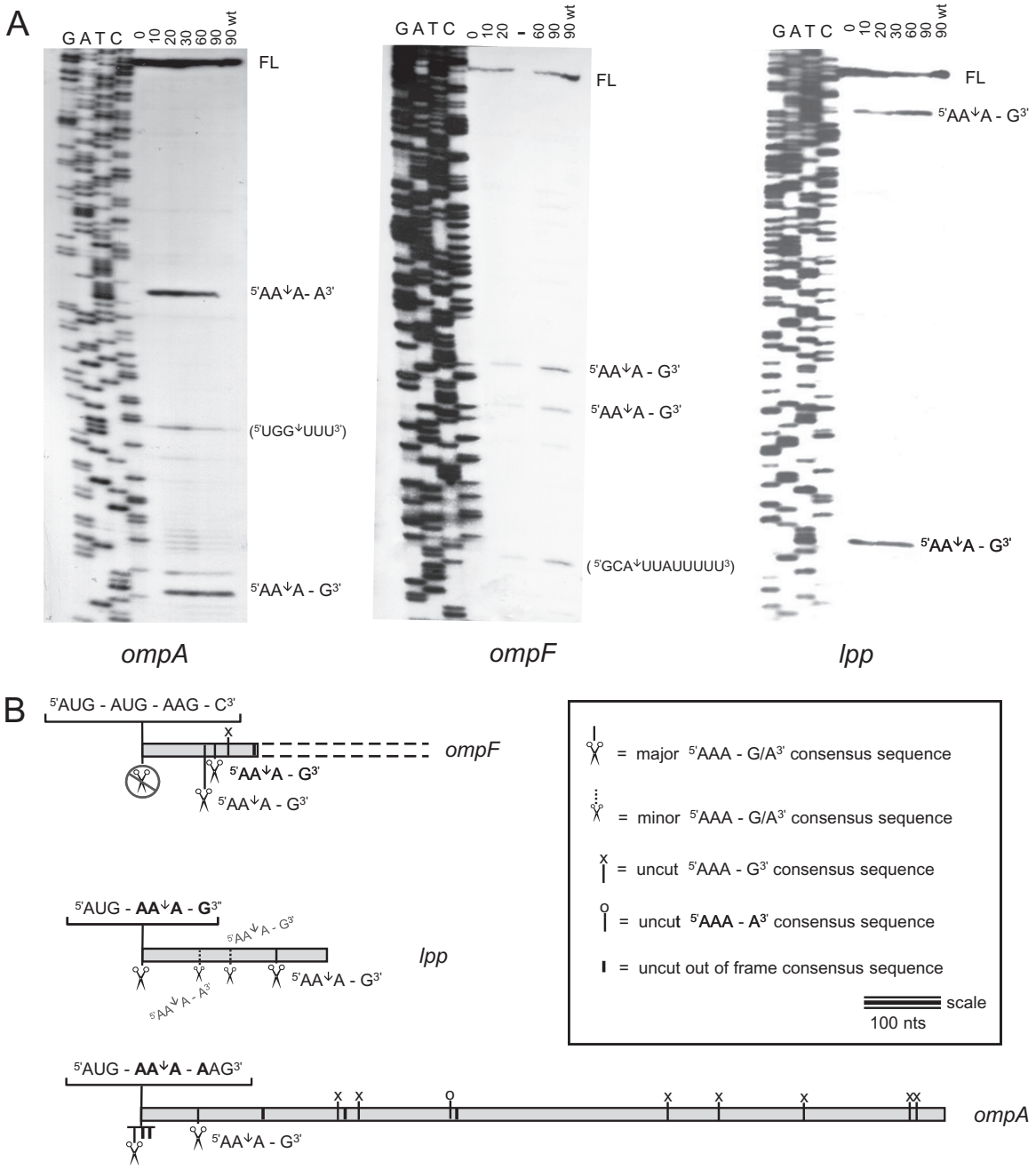

age site maps to the first incidence of the $^{5'}$AAA – G/A$^{3'}$ consensus in the mRNA. For example, the first incidence of the YafQ recognition site maps to the +2 codon for *lpp* and *ompA* mRNAs, and cleavage is detected in the beginning of the transcript. However, *ompF* mRNA begins with the sequence $^{5'}$AUG – AUG – AAG – CGC. . . and therefore does not have the consensus sequence $^{5'}$AAA – G/A$^{3'}$ at +2. Instead, the first of the two major YafQ cleavage sites in *ompF* mapped to the first appearance of the consensus, $^{5'}$AAA – G$^{3'}$, at codon 28. The second major *ompF* cleavage site detected with this primer was also $^{5'}$AAA – G$^{3'}$, and this cut site mapped to the second incidence of the consensus site at codon 32. Therefore, it is not essential that the recognition sequence required for YafQ cleavage begin at the +2 codon of the target mRNA; YafQ instead appears to require the presence of an in-frame $^{5'}$AAA – G/A$^{3'}$ consensus sequence. Finally, longer exposures of the *lpp* primer extensions revealed two minor YafQ-specific cleavage sites – $^{5'}$AA$^{\downarrow}$A – G3′ at codon 40 and a marginally detectable $^{5'}$AA$^{\downarrow}$A – A3′ at codon 27 (Fig. 4B). The latter sequence was underrepresented in our samples, constituting just one of the six major cleavage sites we identified. The reason for inefficient cleavage at some consensus sites that map in between two major cleavage sites is unclear, but may involve interference due to secondary structure or indicate that weak YafQ recognition sequences may be cleaved more efficiently if they are at the +2 codon, just as the ribosome transitions from an initiation complex to an elongating complex.

Finally, comparison of the *in vitro* and *in vivo* activities of YafQ revealed that only one of the six cleavage sites contained the same A-rich consensus site we identified *in vivo*. Therefore, most YafQ cleavage sites on MS2 were not similar to the *in vivo* consensus indicating that the YafQ endoribonuclease exhibits higher sequence specificity *in vivo* upon YafQ binding to the 50S ribosomal subunit and/or other components of the translation machinery.

YafQ interacts with the E. coli *ribosome* in vivo

Of the other two YafQ family member toxins, YoeB and RelE, the mechanism of action of only RelE has been elucidated (Christensen *et al*., 2001; Galvani *et al*., 2001). As RelE functions through the ribosome and the consensus for YafQ cleavage exhibited a preference for in-frame AAA codons, we tested if YafQ also interacted with the ribosome. We first obtained ribosome profiles from control and YafQ-induced *E. coli* cells to determine if YafQ expression altered the profile pattern (Fig. 5). Thirty minutes after YafQ induction (a point where cell growth was completely arrested, Fig. 1A) we consistently observed two anomalies in the ribosome profiles relative to the wild-type control: lower polysome peak heights and the appearance of an additional peak sedimenting at a slightly lower density than the 30S peak. This suggested that the presence of YafQ decreased polysome stability and directly or indirectly altered ribosome structure *in vivo*.

To assess whether YafQ directly interacted with ribosomes or ribosomal subunits, we subjected the ribosome profile fractions from Fig. 5B to Western blotting analysis using a polyclonal antibody to DinJ–YafQ. We detected YafQ predominantly in the 70S fractions, but also in the 50S fractions. YafQ was not detected in either the polysome fractions or the two peaks sedimenting in the 30S region. These results suggested that YafQ interacts with the ribosome through association with the 50S ribosomal subunit. To verify this result, we repeated the ribosome profile analysis under low-magnesium conditions to dissociate the monosome into 50S and 30S particles and demonstrated that YafQ sedimented exclusively with 50S fractions (Fig. 5C). DinJ antitoxin was not associated with the ribosome fractions. In addition, we did not detect free YafQ in the soluble fractions, indicating that most or all of the free YafQ is ribosome-associated. We concluded that YafQ primarily interacts with the 70S monosome *in vivo*, and it appears to be assembled with the monosome through interaction with the 50S ribosomal subunit.

Notably, YafQ was not present in the additional peak that overlapped with the 30S ribosomal subunit peak. When the ribosome profile fractions from YafQ induced cells were silver stained, the protein composition of the 30S ribosomal peak was comparable in both YafQ-induced and uninduced samples. However, while the band intensities of most ribosomal proteins appeared similar in both peaks, some bands were either absent or markedly lighter in the lower density peak (data not shown). Our data suggest that the extra peak comprises a 30S ribosomal subunit precursor that is likely a by-product of a ribosomal maturation defect resulting from the YafQ overexpression. In fact, we later determined that YafQ expression leads to accumulation of 17S rRNA precursor (data not shown), further supporting the notion that YafQ expression somehow perturbs the ribosome maturation process.

YafQ(H87Q) abolishes toxicity but not ribosome binding

We have demonstrated that YafQ mediates sequence-specific and frame-dependent mRNA cleavage at $^{5'}$AAA – G/A$^{3'}$. The potent activity of YafQ *in vitro* (Figs 2A and 3) suggests that it mediates mRNA cleavage while it is associated with the ribosome, which acts as a platform to *deliver* YafQ to the mRNA and *position* it in a manner to impart precision such that mRNA is cleaved at the ribosomal A site when $^{5'}$AAA – G/A$^{3'}$ is encountered within the first ~60 codons. However, there is a formal possibility that

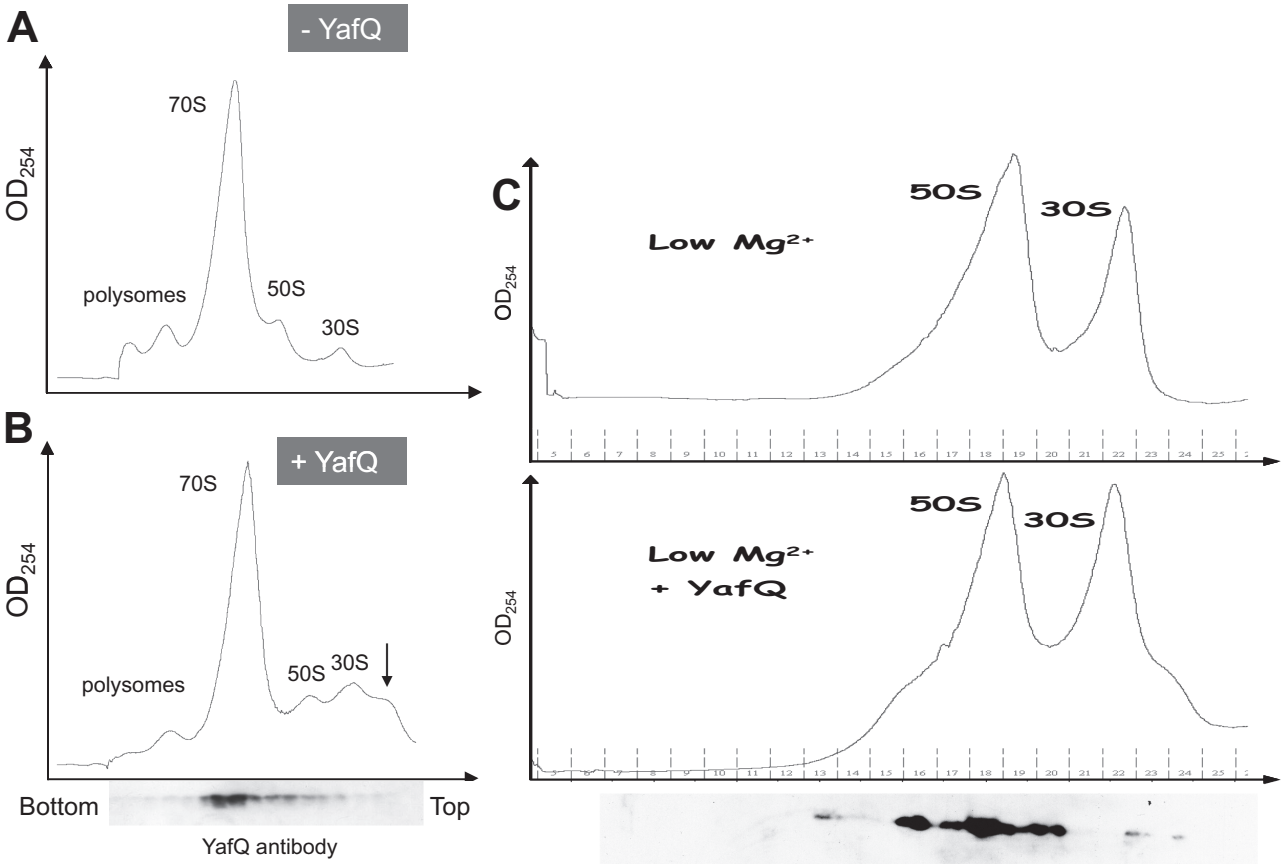

Fig. 5. YafQ associates with the ribosome *in vivo*.
A and B. Ribosome profiles of BW25113[YafQ-pBAD22] cells with (+YafQ) or without (–YafQ) induction with 0.2% arabinose; the extra peak sedimenting above the 30S fraction when YafQ is expressed is highlighted with an arrow.
C. YafQ associates with the 50S ribosomal subunit. YafQ Western blot lanes in B and C are aligned to their respective fraction number on the profiles above.

YafQ enhances the intrinsic mRNA cleavage activity of the ribosome (Hayes and Sauer, 2003) as suggested for RelE (Pedersen *et al*., 2003). To help differentiate whether the cleavage activity of the YafQ associated-ribosome complex is due to YafQ or the ribosome (by YafQ-mediated enhancement of the intrinsic cleavage activity of the ribosome) we attempted to create a catalytically inactive form of YafQ. Comparison of the protein sequence of YafQ to its two family members revealed that histidine 87 of YafQ aligned to the highly conserved arginines in RelE and YoeB known to be important for toxin activity (Motiejunaite *et al*., 2007). Therefore, we constructed a YafQ(H87Q)-pBAD33 plasmid and examined the growth rate upon induction of YafQ(H87Q). Unlike wild-type YafQ, induction of YafQ(H87Q) no longer resulted in growth arrest (Fig. 6A), indicating that this single amino acid substitution abolished YafQ-mediated toxicity. We then performed a series of Northern blots for *ompA* and *lpp* transcripts to check whether YafQ(H87Q) expression led to mRNA degradation. mRNA was no longer degraded upon expression of YafQ(H87Q) (Fig. 6B), indicating that this mutant had lost the ability to cleave mRNA, accounting for its non-toxic phenotype.

To distinguish whether the loss of mRNA cleavage was due to a loss of YafQ(H87Q) enzymatic activity or due to an inability of the mutant to bind to ribosome and possibly enhance intrinsic ribosomal cleavage activity, we repeated our ribosome profile analyses with extracts from YafQ(H87Q)-induced cells. Strikingly, both characteristic features of YafQ toxicity on the ribosome profile were now absent: polysome levels were not diminished, nor did we observe the additional peak sedimenting adjacent to the 30S peak (Fig. 6C and D). Finally, to test whether YafQ(H87Q) retained its ability to associate with the ribosome, we subjected the fractions from the YafQ(H87Q)-induced panel to Western blotting analysis. YafQ(H87Q) retained its ability to interact with both the 70S and 50S particles (Fig. 6D).

In conclusion, the YafQ(H87Q) mutant data suggest that: (i) the lack of a toxic phenotype for the mutant was

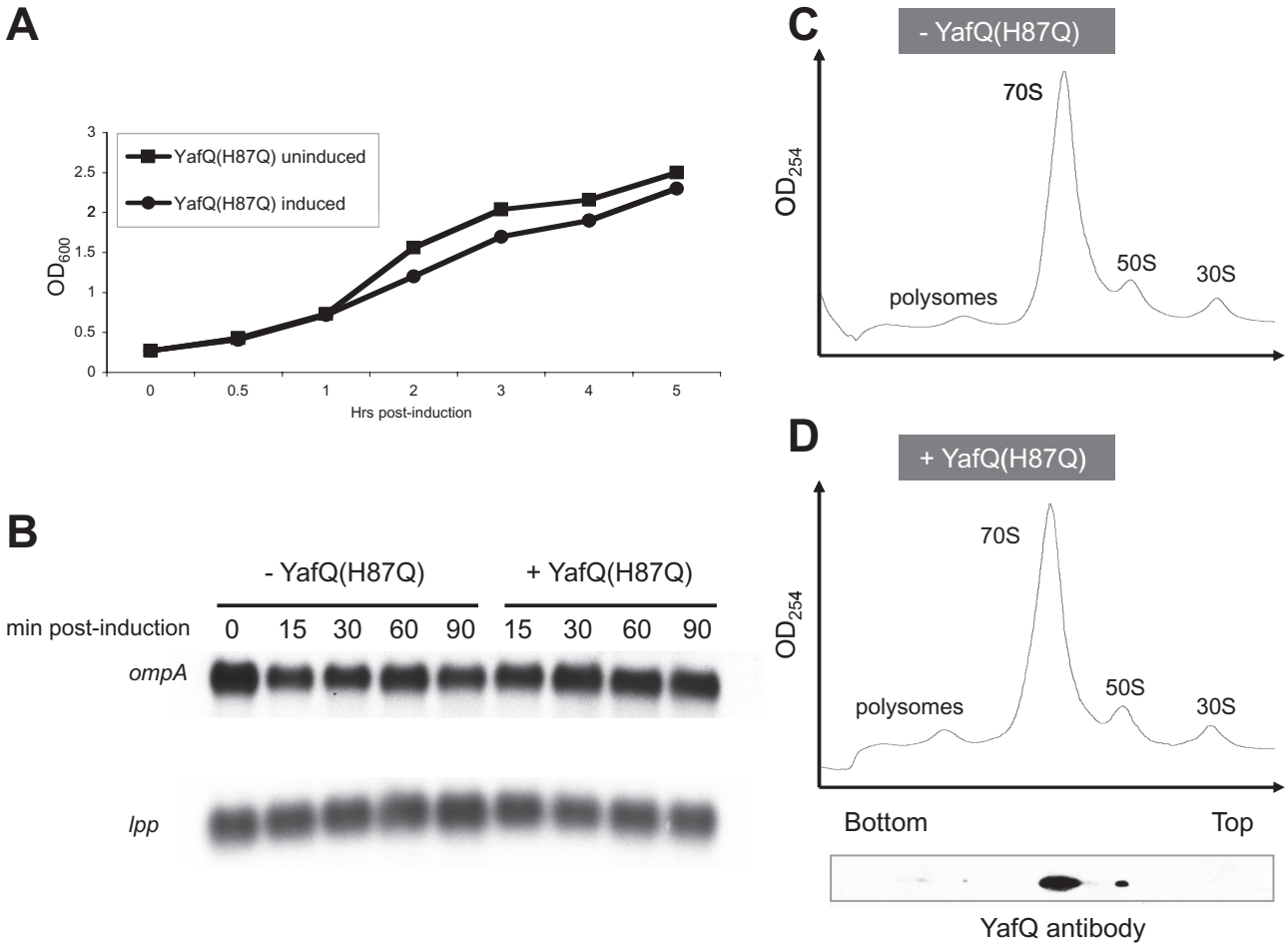

Fig. 6. YafQ(H87Q) expression results in loss of toxicity (A) and mRNA cleavage (B) but not ribosome binding (C and D); the characteristic extra peak in the 30S region is also absent. The growth profile was repeated twice, both times yielding a similar result.

due to loss of the enzymatic activity of YafQ(H87Q) and not due to its inability to bind the ribosome; (ii) YafQ does not enhance the intrinsic mRNA cleavage activity of the ribosome; (iii) YafQ mediates sequence-specific and frame-dependent mRNA cleavage and the ribosome serves to deliver YafQ to the mRNA; and (iv) H87 is essential for the catalytic activity of YafQ. The notion that the endoribonuclease activity exhibited by the YafQ-ribosome complex is derived from YafQ is substantiated by our data demonstrating that purified YafQ was able to cleave RNA *in vitro* (Fig. 2A).

LexA and the DinJ–YafQ complex bind to the dinJ–yafQ *palindrome*

Although MazEF and RelBE have been implicated in the stringent response (Masuda *et al.*, 1993; Aizenman *et al.*, 1996; Christensen and Gerdes, 2003; 2004; Pedersen *et al.*, 2003), in general, the physiological roles and specific triggers of individual TA module transcription are not well understood (Tsilibaris *et al.*, 2007). Palindromes are characteristically present in TA module promoters – they are bound by the TA complex or the antitoxin alone to autoregulate the operon (Gerdes *et al.*, 2005). The palindrome upstream of *dinJ–yafQ* is unique among known *E. coli* proteic TA modules because this sequence has similarity to a consensus LexA binding site (Lewis *et al.*, 1994; Fernandez De Henestrosa *et al.*, 2000), suggesting that this module is regulated by DNA damage (Fig. 7A). In fact, for many years its physiological significance was dismissed because electrophoretic mobility shift assay (EMSA) and Northern experiments published in did not show a LexA gel shift nor support LexA regulation of *dinJ–yafQ* respectively (Fernandez De Henestrosa *et al.*, 2000).

We used an EMSA assay to determine if DinJ–YafQ(His)$_6$ was able to bind to a dsDNA fragment corresponding to the upstream palindrome sequence of the *dinJ–yafQ* module (Fig. 7A). DinJ–YafQ(His)$_6$ complex was able to bind its upstream palindrome, supporting a role for this TA complex in autoregulation characteristic of

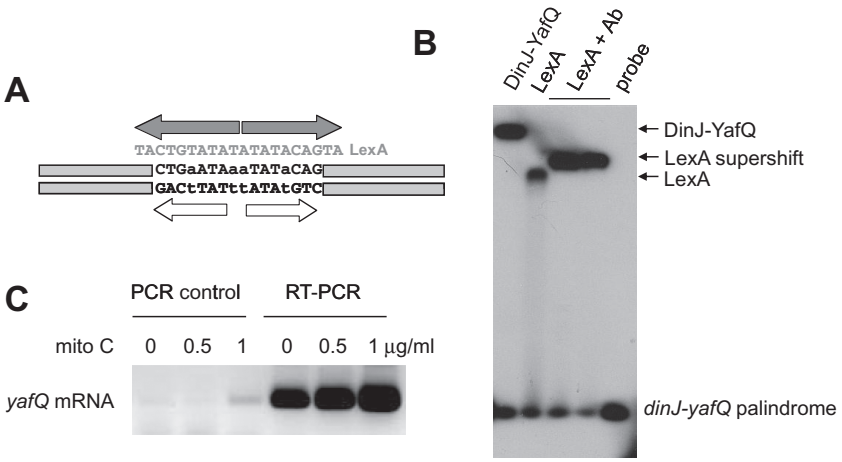

Fig. 7. LexA regulation of *dinJ–yafQ*.
A. Schematic of the *dinJ–yafQ* palindrome positioned at –16 to –33 from the translation start site (imperfect repeat; mismatched residues in lowercase) relative to the LexA box; arrows indicate axes of symmetry of repeated sequences.
B. EMSA demonstrating LexA or DinJ–YafQ complex binding to the *dinJ–yafQ* palindrome.
C. *yafQ* is induced upon DNA damage in wild-type cells. RT-PCR after mitomycin C treatment; PCR control reflects the amount of PCR product amplified from an equivalent amount of total RNA preparation used in the RT-PCR (negligible relative to the RT-PCR signals in the three right hand lanes) obtained from the same quantity of total RNA subjected to RT-PCR. Equivalent samples loaded in each lane; reaction products (stained with EtBr) shown as a negative exposure.

TA modules. LexA(His)$_6$ was also able to bind the *dinJ–yafQ* palindrome, and this binding was supershifted by the addition of a LexA antibody (Fig. 7B), consistent with recent genome-wide *in vivo* chromatin immunoprecipitation experiments (Wade *et al*., 2005). We did not observe LexA(His)$_6$ binding to the *relBE* palindrome (data not shown) which suggested that (i) the binding of LexA to the *dinJ–yafQ* palindrome we observed was specific to the *dinJ–yafQ* module and (ii) the *in vivo* regulation of *dinJ–yafQ* is likely distinct from its family members. Demonstration of either LexA or the DinJ–YafQ binding to the LexA box upstream of the *dinJ–yafQ* module also suggests that competition occurs and both contribute to its repression and autoregulation.

The LexA repressor plays a central role in initiating the SOS response upon DNA damage (Shinagawa, 1996), suggesting that regulation of *dinJ–yafQ* transcription is also linked to DNA damage. We exposed wild-type cells to increasing levels of mitomycin C (an antibiotic that acts by alkylation of DNA leading to cross-linking of complementary strands), purified total RNA, and performed a reverse transcription polymerase chain reaction (PCR) to determine if the induction of DNA damage by mitomycin C affected the steady-state levels of *dinJ and yafQ* mRNAs. Our results revealed a modest, but consistent, increase in the steady-state mRNA levels of *yafQ* (Fig. 7C) but not *dinJ* (data not shown) in wild-type cells after mitomycin C treatment. Our findings are consistent with microarray analysis of *E. coli* transcripts after UV treatment (Courcelle *et al*., 2001). The steady-state level of *dinJ* was unchanged while levels of *yafQ* increased less than twofold. In fact, many SOS response genes are not upregulated more than twofold.

Next, we examined if a Δ*dinJ–yafQ E. coli* strain exhibited differences in recovery after induction of DNA damage relative to wild-type cells. We employed two standard methods, exposure to UV irradiation and mitomycin C treatment. Using several standard protocol variations (time, concentration and media) for mitomycin C treatment, we did not observe a consistent and substantial difference in recovery of colony forming units between the wild type and Δ*dinJ–yafQ* strain (data not shown).

Discussion

Free-living bacterial cells are equipped with a remarkable repertoire of stress survival mechanisms. Although the physiological role of chromosomal TA systems/modules is somewhat controversial (Tsilibaris *et al*., 2007), the majority of evidence supports the hypothesis whereby they enhance cell survival during and after short pulses of stress routinely encountered when free-living bacteria exist in their native environments. It is also possible that TA systems are instrumental in the elimination of cells damaged after stress conditions to maintain a healthy population of cells (Engelberg-Kulka *et al*., 2004; 2006). In this work, we have presented evidence that the *E. coli* chromosomally encoded operon at the *dinJ–yafQ* locus constitutes a genuine TA module and uncovered the mechanism of action of the YafQ toxin.

Northern analysis revealed rapid and complete degradation of three mRNA transcripts upon YafQ expression,

and Western analysis demonstrated sedimentation of YafQ with 70S monosomes and the 50S ribosomal subunit. Therefore, YafQ targets the cellular population of actively translating mRNA for cleavage through interaction with the ribosome (mRNA synthesis and translation are coupled in bacteria, precluding the existence of free, intact mRNAs). Primer extension analyses enabled the identification of a reading frame-dependent recognition sequence for YafQ cleavage, $^{5'}$AAA – (G/A)$^{3'}$. The primary YafQ cleavage site was at the same position (codon +2) for two independent transcripts (*lpp* and *ompA*), i.e. $^{5'}$ATG – AAA – (G/A)XX$^{3'}$. Interestingly, *ompF* lacked the consensus in the beginning of the transcript and, as a consequence, no major cleavage was detected at position +2. However, we mapped both major cleavage sites to the first and second incidence of the in-frame $^{5'}$AAA – (G/A)$^{3'}$ sequence. Although we used primers that covered most of *ompF*, and all of *ompA* and *lpp* (except for the 3′ ends where primer annealed), we did not detect major cleavage products beyond 60 codons/180 nucleotides from the translation start.

Translation initiation is thought to be the rate-limiting step in protein synthesis and several ways of regulating it are employed. Here we demonstrate that ribosome-associated YafQ instead targets the elongation phase. In some cases YafQ acts just after transition of the initiation complex to an elongation complex by cleaving mRNA at its +2 codon (when the initiator codon is bound to the P site and the second codon is positioned at the A site). When the consensus cleavage sequence is not represented early in the mRNA, YafQ appears to remain associated with the ribosome because cleavage occurs once the translation apparatus reaches an in-frame recognition sequence further downstream.

What is the fate of the mRNA transcript after YafQ cleavage *in vivo*? Northern analysis demonstrated a rapid and complete degradation of *lpp*, *ompA* and *ompF* mRNAs upon YafQ induction; primer extension analyses revealed only two major cut sites near the 5′ end (within 180 nucleotides) of all three mRNAs. We can reconcile these results by proposing that cleavage is only detected early in the mRNA because YafQ generally cleaves mRNA with high efficiency. Therefore, from the total pool of a specific mRNA (such as *ompA*), most or all of those mRNAs that were not cleaved at their first consensus sequence, are then cut at the second recognition site by the YafQ-containing elongation complex. As mentioned earlier, subsequent degradation of mRNAs cut by YafQ is likely accelerated by the cellular mRNA degradation machinery (Carpousis, 2007). The extremely rapid rate of mRNA degradation documented by Northern analysis also suggests that mRNA cleaved by YafQ is released from the ribosome (and the protection from degradation it provides) after cleavage. A released transcript would also allow the recycling of ribosomes and tRNAs so they can be directed to translation of SOS response mRNAs (if YafQ involvement in the SOS response is definitively demonstrated in the future).

Interestingly, the AAA codon is the most common codon at +2 in *E. coli*, represented in approximately 10% of all mRNAs containing AUG or GUG start codons (Stenstrom *et al*., 2001). Some reports have also correlated AAA at +2 with high translation initiation efficiency (Stenstrom *et al*., 2001; Brock *et al*., 2007). Purine-rich sequences, especially adenine-rich ones, are correlated with single-strand regions in 16S rRNA (Wang and Hickey, 2002), so it is thought that this may contribute to higher translational efficiency when A-rich sequences are found 3′ of the translation start site. The presence of the AAA codon at +2 is also overrepresented in secretory proteins (Zalucki *et al*., 2007), consistent with its presence in the *ompA* mRNA we studied. Therefore, the YafQ cleavage recognition site may represent an adaptation designed to target the maximal number of transcripts for degradation given the finite levels of free YafQ toxin available under physiological stress (perhaps SOS) conditions.

There are fundamental mechanistic differences between YafQ and its family member RelE. RNA cleavage by RelE is observed in cell-free extracts, but not with purified RelE protein combined with RNA. Therefore, the cleavage activity attributed to RelE has been attributed to the endonucleolytic activity of the ribosome (Hayes and Sauer, 2003; Pedersen *et al*., 2003; Sunohara *et al*., 2004a,b). In contrast, we demonstrated that YafQ exhibits RNA cleavage activity *in vitro*, with some degree of sequence specificity at low enzyme/substrate ratios. These data are further supported by our identification of a key catalytic residue of YafQ, H87, whose substitution with a glutamine residue abolishes mRNA cleavage and toxicity but does not interfere with the association of YafQ and the ribosome. This feature makes YafQ unique among *E. coli* TA toxins and distinct from family member RelE.

Based on our findings, we propose the following model of YafQ activity in *E. coli* cells. DinJ–YafQ is expressed as a stable protein complex from the *dinJ–yafQ* locus. DinJ is degraded by proteases after the physiological switch is triggered (currently unknown, possibly the SOS response), leaving YafQ free to interact with 70S ribosomes or free 50S ribosomal subunits. YafQ induces cleavage of the mRNA transcript at the frame-dependent $^{5'}$AAA – G/A$^{3'}$ recognition site until the mRNA pool is depleted. mRNA cleavage efficiency must be high because YafQ-mediated cleavage was not documented past the 60th codon, even in mRNAs composed of > 300 codons. Depletion of the mRNA pool also occurs quickly, because steady-state mRNA levels drop rapidly to unde-

tectable levels. Finally, YafQ mRNA cleavage leads to growth arrest because these transcripts (including those encoding essential proteins) are not translated.

Although the *dinJ–yafQ* operon is regulated by LexA, the role of this module in the SOS response is unclear because we did not detect differences in recovery of colony forming units after UV stress or mitomycin C treatment of the Δ*dinJ–yafQ* strain compared with wild type. Another gene pair that appears to be a TA system, *yafN–yafO*, is harboured within the *dinB–yafN–yafO–yafP* operon and is just downstream of *dinJ–yafQ* (McKenzie *et al*., 2003). *dinB* (encoding DNA polymerase IV) is strongly induced (7.7-fold) after UV treatment, as are the *yafN* antitoxin and *yafO* toxin genes, 2.7- and 3.6-fold respectively (Courcelle *et al*., 2001). TA system antitoxins are susceptible to proteases induced upon stress, and our data suggest that DinJ is targeted by both Lon and ClpXP (Fig. 1D); therefore, YafQ toxin should be in excess after UV stress. As TA toxins act by reversibly inhibiting cell growth, YafQ is implicated in facilitating the temporary growth arrest that is required to repair DNA (Opperman *et al*., 1999). However, the functions of TA toxins YafQ and YafO may be redundant because checkpoint control after DNA damage (Opperman *et al*., 1999) is crucial to maintenance of genome integrity, so when analysing the response to stress using the Δ*dinJ–yafQ* strain, possible YafQ involvement in DNA damage checkpoint control may be masked by the presence of functional YafO. In fact, in addition to being regulated by LexA, two features of YafQ-mediated growth arrest are consistent with its involvement in the SOS response. First, some translation still occurs when YafQ fully arrests growth (Fig. 1E), in contrast to the growth arrest facilitated by other TA toxins that comprehensively degrade mRNA (e.g. MazF and ChpBK). The SOS response requires some level of transcription to activate the 50 plus LexA regulated genes. Second, steady-state transcript levels of *yafQ* increase after exposure to DNA damaging agent mitomycin C (Fig. 7C; Courcelle *et al*., 2001); LexA and RNA polymerase occupancy at the *dinJ–yafQ* LexA box using chromatin immunoprecipitation-chip analysis revealed the loss of LexA binding and a twofold increase in RNA polymerase occupancy after UV irradiation (Wade *et al*., 2005). More detailed analyses of YafQ targets and elucidation of YafO function should shed light on the significance of LexA regulation of the operons containing these two TA toxins.

Experimental procedures

Strains, plasmids and reagents

The *E. coli* strains *BL21(DE3)* (F- *omp*T *hsd*S_β(r_β-m_β-) *dcm gal* (DE3) tonA) (Novagen), and BW25113 (*lacI*^{q}*rrnB*$_{T14}$ Δ*lacZ*$_{WJ16}$ *hsdR514* Δ*araBAD*$_{AH33}$ Δ*rhaBAD*$_{LD78}$) (Datsenko and Wanner, 2000) were used for all protein expression and toxicity studies. *E. coli* K-12 Mach1 T1 cells (Δ*rec*A1398 *end*A1 *ton*A Φ80Δ*lac*M15 Δ*lac*X74 *hsd*R ($r_K^-m_K^+$)) (Invitrogen) were used for all cloning experiments throughout the section. *E. coli* K-12 *DH5α* (F⁻ Φ80d*lac*ZΔM15 Δ(*lac*ZYA-*arg*F) U169 *rec*A1 *end*A1 *hsd*R17 (r_K^+, m_K^+) *pho*A *sup*E44 λ⁻*thi*-1 *gyr*A96 *rel*A1) genomic DNA served as the PCR template to clone out the *dinJ–yafQ* module, *yafQ*, *dinJ* and *lexA*. The *E. coli* BW25113 strains that carried deletions of the *mazEF*, *chpBIK*, *relBE*, *yefM–yoeB* and *dinJ–yafQ* modules (BW25113 Δ6 or just Δ6 in text) were generous gifts from Qian Tan and Yoshi Yamaguchi of the Inouye laboratory. The *E. coli* BW25113 strains that carried individual deletions of the *lon*, *clpP*, *clpA* or *clpX* loci were also generous gifts of the Inouye lab. Plasmids used in this study are listed in Table 1. All bacterial liquid cultures were grown in Luria Broth (LB) media at 37°C, unless otherwise noted. The working concentrations of ampicillin and chloramphenicol were 34 μg ml^{-1} and 25 μg ml^{-1} respectively. The DNA sequences of PCR fragments used for cloning were confirmed by automated DNA sequence analysis. Polyclonal antibodies used for Western analysis were raised to the DinJ–YafQ complex (Pocono Rabbit Farm and Laboratory).

Table 1. Plasmids.

Name	Description
dinJ-yaf-pET21c	*dinJ–yafQ* module in pET21c (5′NdeI/XhoI3′)
dinJ-yaf(His)$_6$-pET21c	*dinJ–yafQ* module (His)$_6$-tagged in pET21c (5′NdeI/XhoI3′)
dinJ–yafQ-pBAD33	*dinJ–yafQ* module in pBAD33 (5′XbaI/HindIII3′)
yafQ-pBAD33	*yafQ* in pBAD33 (5′XbaI/HindIII3′)
yafQ-pET21c	*yafQ* in pET21c (5′NdeI/EcoRI3′)
dinJ-pINIII	*dinJ* in pINIII (5′EcoRI/BamHI3′)
lexA-pET21c	*lexA* in pET21c (5′NdeI/BamHI3′)
lexA(His)$_6$-pET21c	*lexA* (His)$_6$-tagged in pET21c (5′NdeI/XhoI3′)

Antitoxin stabilization assays

E. coli BW25113, Δ*lon*, Δ*clpP*, Δ*clpA* and Δ*clpX* cells harbouring *dinJ*-pINIII were grown in LB media to mid-exponential phase (OD_{600} = 0.3–0.4). Cultures were then induced with 1 mM IPTG for a period of 10 min before treatment with 150 μg ml^{-1} Hygromycin B. Aliquots were taken from each strain at 0, 0.5, 1, 2, 3, 4 and 5 h post induction, and cellular lysates were run on a 15% SDS-PAGE gel followed by Western blotting analysis.

Recombinant DinJ and YafQ

The *dinJ–yafQ*(His)$_6$-pET21c and *lexA*(His)$_6$-pET21c constructs were transformed into BL21(DE3) cells, and induced with 1 mM IPTG for a period of 4 h. Cells were lysed using a French Press, and the protein extracts were applied to a Ni-NTA resin (Qiagen). The columns were washed with wash buffer containing 20 mM imidazole, and each protein was eluted from the column with buffer containing 250 mM imidazole.

To separate the respective components of the DinJ–YafQ protein complex, the complex was denatured with 6 M guanidine-HCl and applied to an Ni-NTA column, resulting in the release of purified DinJ from the complex and the retention of YafQ(His)$_6$ on the Ni-NTA resin. The bound YafQ(His)$_6$ was eluted as described above, and renatured in a stepwise manner using Slide-A-Lyzers (Pierce Biotechnology) as previously described (Zhang *et al*., 2003).

Protein synthesis in vitro *and* in vivo

BW25113 cells containing *yafQ*-pBAD33 were assayed for defects in translation *in vitro* using toluene-treated cells as previously described (Halegoua *et al*., 1976a,b). For *in vivo* studies, a 100 ml culture of BW25113 cells containing *yafQ*-pBAD33 was grown at 37°C in M9 medium (with 0.5% glycerol and 1 mM of all amino acids except cysteine and methionine) until the OD_{600} reached 0.3. The culture was then split into two 50 ml cultures, and a final concentration of 0.2% arabinose was added to one, while an equal volume of sterile H_2O was added to the other. 600 μl aliquots were removed at 0, 30, 60, 90 and 120 min post induction and incubated with 30 μCi [^{35}S]-methionine at 37°C. After a 1 min incubation, the reaction was stopped, and the rate of protein synthesis was determined via scintillation counting as previously described (Zhang *et al*., 2003).

Analysis of steady-state mRNA levels

E. coli BW25113 cells containing *yafQ*-pBAD33 or *yafQ(H87Q)*-pBAD33 were grown in LB media at 37°C. When the OD_{600} value reached 0.4, the culture was split into equal portions and arabinose was added to one at a final concentration of 0.2%, while an equal volume of water was added to the other as a control. Culture samples were harvested at 0, 10, 20, 30, 60 and 90 min post induction. Total RNA was extracted using the hot phenol method as previously described (Sarmientos *et al*., 1983). The radiolabelled DNA fragments used for hybridization to the Northern blots were generated via PCR of the full-length open reading frames of the *E. coli* genes *ompA*, *ompF* and *lpp*.

Determination of YafQ ribonuclease activity in vitro

Total cellular RNA was isolated from BW25113 cells as described above. Ten micrograms of total RNA was added to a reaction containing 10 mM Tris pH 7.8, and increasing amounts of YafQ(His)$_6$ and DinJ for a total reaction volume of 10 μl. YafQ(His)$_6$ and DinJ were pre-incubated together for 10 min at room temperature prior to starting the reaction. The reaction was allowed to proceed for 15 min at 37°C, and samples were run on a 3.5% acrylamide gel and stained with ethidium bromide.

The YafQ MS2 cleavage assays were carried out as described by Zhu *et al*. (2006). Full-length MS2 RNA was partially digested with or without purified toxin protein YafQ, and with or without purified CspA protein at 37°C for 15 min. DinJ antitoxin was also added to demonstrate that the cleavage activity observed was due to YafQ and not a contaminating ribonuclease. The digestion reaction mixture (10 μl total volume) consisted of 0.8 μg of MS2 RNA substrate, 31.25 ng of YafQ, 1 μg of DinJ, 32 μg of CspA and 0.5 μl of RNase inhibitor (Roche) in 10 mM Tris-HCl (pH 7.8). Primer extensions were carried out at 47°C for 1 h in a 20 μl reaction mixture as described previously (Zhang *et al*., 2005a). CspA was purified as described previously (Chatterjee *et al*., 1993). The reactions were stopped by the addition of 12 μl of sequence loading buffer (95% formamide, 20 mM EDTA, 0.05% bromphenol blue and 0.05% xylene cyanol EF). The samples were incubated at 90°C for 5 min prior to electrophoresis on a 6% polyacrylamide 6 M urea gel. The primers were 5′-labelled with [^{32}P]-ATP using T4 polynucleotide kinase. The primers used were L2, 5′-CCTATCAA GGGTACTAAAAG-3′ (Fig. 3A); D, 5′-CCGCTCTCAGAG CGCGGGGG-3′ (Fig. 3E–F); B, 5′-CAAATCGGGAGA ATCCCGGG-3′ (Fig. 3C–D); and E1, 5′-TGCATTGCCTTAA CAATAAG-3′ (Fig. 3B).

Primer extension analysis

E. coli BW25113 or BW25113 Δ6 cells carrying *yafQ*-pBAD33 were grown in LB media at 37°C. When the OD_{600} value reached 0.4, the culture was split and arabinose was added to one at a final concentration of 0.2%, while an equal volume of water was added to the other as a control. Culture samples were removed at 0, 10, 30, 60 and 90 min post induction, and total RNA was extracted as described above. Primer extensions in Fig. 4 were carried out using radioactively labelled primers as previously described (*ompA2*: 5′-CGGGCCATT GTTGTTGATGAAACC-3′; *ompF*: 5′-AAACCAAGACGGGCA TAGGTC-3′; *lpp*: 5′- TTACTTGCGGTATTTAGTAGCC-3′ (Zhang *et al*., 2003). Five other *ompA* primers were also used to detect cleavage products throughout the mRNA: *ompA1*, 5′-CAGTGTACCAGGTGTTATCTT-3′; *ompA3*, 5′-GGGTAA CCCAGTTTAGCGGTCAGTTG-3′; *ompA4*, 5′-ACACCCA GGCTCAGCATGCCGTTGTCC-3′; *ompA5*, 5′-TCAGAAC CGATGCGGTCGGTGTAACCC-3′; *ompA6*, 5′-GCTGAGTTA CAACGTCTTTGATACC-3′.

The DNA sequencing ladder used to assess cleavage sequences was prepared with a Sequenase Version 2.0 DNA Sequencing Kit (USB) using the respective oligonucleotides for primer extension reactions. The sequencing ladder and the primer extension products were separated on a 6% polyacrylamide/8 M urea sequencing gel and visualized by autoradiography.

Ribosome profile analysis

E. coli BW25113 cells containing *yafQ*-pBAD33 or *yafQ(H87Q)*-pBAD33 were grown in 200 ml of LB media at 37°C. At an OD_{600} of 0.4, the culture was split into two flasks of 50 ml each. Arabinose was added to a final concentration of 0.2% for one of the cultures. After 30 min, cells were pelleted at 15 000 r.p.m. for 20 min in a Sorvall SA-600 rotor and resuspended in 1 ml of polysome profile buffer (p.p.b.; 10 mM Tris pH 7.5, 50 mM NH_4Cl, 10 mM $MgCl_2$, 5 mM DTT). Cells were frozen in liquid nitrogen and thawed on ice, and 10 μl of 10 mg ml^{-1} lysozyme (Sigma) was added to each sample. Five additional freeze-thaw steps were performed and 150 μl of the resulting extract was layered onto a 5–40%

sucrose gradient in p.p.b and centrifuged at 35 000 r.p.m. for 3 h at 4°C in a Beckman SW41 rotor. Gradients were fractionated and collected (400 μl each) with continuous monitoring at 254 nm. Aliquots of each fraction collected were run on a 15% SDS-PAGE gel and either silver stained or subjected to Western blotting analysis.

Electromobility gel shift assays

Electrophoretic mobility shift assays were performed essentially as described (Golemis and Brent, 1992). Briefly, complementary oligonucleotides (5′-CA**AGCTGAATAAA TATACAGCA**CAGGTACCCCA-3′ and its complement) of the 5′ sequence upstream of the open reading frame of *dinJ* were synthesized (the proposed regulatory upstream palindrome is in bold-face type), annealed at 65°C for 2 min and allowed to cool to room temperature overnight. The annealed oligonucleotides were radiolabelled and incubated with purified protein (either DinJ–YafQ$(His)_6$, DinJ, YafQ$(His)_6$, or LexA-$(His)_6$) for 30 min at 30°C in the reaction buffer (4% glycerol, 1 mM EDTA, 10 mM Tris HCl pH 7.6, 5 mM $CaCl_2$, 100 mM NaCl, 10 mM β-ME). LexA antibody (a generous gift from Erica Golemis, Fox Chase Cancer Center) was added to the LexA reactions to demonstrate LexA binding specificity. EMSA reactions were run on a native 6% polyacrylamide gel and visualized by autoradiography.

Reverse transcriptase-PCR

E. coli BW25113 cells were grown in LB media until exponential phase (OD_{600} = 0.3–0.4). Mitomycin C (or an equal volume of water) was added to the growing culture in a range of concentrations from 0 μg ml^{-1} to 1 μg ml^{-1}, and allowed to incubate for 1 h. Total RNA was isolated from these cultures as described above, and reverse transcriptase reactions were carried out on equal amounts of total RNA as described above with *yafQ* primer 5′-CGGAATTCTTACCCAAA GAGCGC-3′. The reverse transcriptase was then heat inactivated for 10 min at 75°C, and all samples were treated with DNase-free RNase for 10 min. These reactions were then used as template for the PCR reaction using the following primers to amplify full-length *yafQ*, 5′-GGAATTCCATAT GATGATTCAAAGGGATATTG-3′ and 5′-CGGAATTCTTAC CCAAAGAGCGC-3′. PCR reactions were then run on 0.8% agarose gels and stained with ethidium bromide.

Acknowledgements

This work was funded in part by RO1 Grant GM 74097 from the National Institutes of Health (NIH) to N.A.W., the Northeast Structural Genomics Consortium U54 grant (GM74958) entitled Structural Genomics of Eukaryotic Domain Families (Gaetano Montelione-Rutgers University, PI; M.I. and N.A.W. are subproject PI and Co-PI respectively) from the NIH and Takara Bio, Inc. Angela Cook was partially supported by the Bernard Koft-Wayne Umbreit fellowship from the Microbiology and Molecular Genetics Graduate Program at Rutgers University. Meredith H. Prysak was supported by the T32 Training Grant, Virus–Host Interactions in Eukaryotic Cells AI07403 from the NIH-NIAID awarded to Sidney Pestka.

Note Added in Proof

A manuscript describing the mechanism of action of *E. coli* YoeB was accepted for publication in *J Biol Chem* while this work was in the proof stage.

References

Aizenman, E., Engelberg-Kulka, H., and Glaser, G. (1996) An *Escherichia coli* chromosomal ‘addiction module’ regulated by guanosine [corrected] 3′,5′-bispyrophosphate: a model for programmed bacterial cell death. *Proc Natl Acad Sci USA* **93:** 6059–6063.

Brock, J.E., Paz, R.L., Cottle, P., and Janssen, G.R. (2007) Naturally occurring adenines within mRNA coding sequences affect ribosome binding and expression in *Escherichia coli*. *J Bacteriol* **189:** 501–510.

Carpousis, A.J. (2007) The RNA degradosome of *Escherichia coli*: an mRNA-degrading machine assembled on RNase E. *Annu Rev Microbiol* **61:** 71–87.

Chatterjee, S., Jiang, W., Emerson, S.D., and Inouye, M. (1993) The backbone structure of the major cold-shock protein CS7.4 of *Escherichia coli* in solution includes extensive beta-sheet structure. *J Biochem (Tokyo)* **114:** 663–669.

Christensen, S.K., and Gerdes, K. (2003) RelE toxins from bacteria and Archaea cleave mRNAs on translating ribosomes, which are rescued by tmRNA. *Mol Microbiol* **48:** 1389–1400.

Christensen, S.K., and Gerdes, K. (2004) Delayed-relaxed response explained by hyperactivation of RelE. *Mol Microbiol* **53:** 587–597.

Christensen, S.K., Mikkelsen, M., Pedersen, K., and Gerdes, K. (2001) RelE, a global inhibitor of translation, is activated during nutritional stress. *Proc Natl Acad Sci USA* **98:** 14328–14333.

Christensen, S.K., Pedersen, K., Hansen, F.G., and Gerdes, K. (2003) Toxin-antitoxin loci as stress-response-elements: ChpAK/MazF and ChpBK cleave translated RNAs and are counteracted by tmRNA. *J Mol Biol* **332:** 809–819.

Christensen, S.K., Maenhaut-Michel, G., Mine, N., Gottesman, S., Gerdes, K., and Van Melderen, L. (2004) Overproduction of the Lon protease triggers inhibition of translation in *Escherichia coli*: involvement of the *yefM-yoeB* toxin-antitoxin system. *Mol Microbiol* **51:** 1705–1717.

Correia, F.F., D’Onofrio, A., Rejtar, T., Li, L., Karger, B.L., Makarova, K., *et al.* (2006) Kinase activity of overexpressed HipA is required for growth arrest and multidrug tolerance in *Escherichia coli*. *J Bacteriol* **188:** 8360–8367.

Courcelle, J., Khodursky, A., Peter, B., Brown, P.O., and Hanawalt, P.C. (2001) Comparative gene expression profiles following UV exposure in wild-type and SOS-deficient *Escherichia coli*. *Genetics* **158:** 41–64.

Datsenko, K.A., and Wanner, B.L. (2000) One-step inactivation of chromosomal genes in *Escherichia coli* K-12 using PCR products. *Proc Natl Acad Sci USA* **97:** 6640–6645.

Ehretsmann, C.P., Carpousis, A.J., and Krisch, H.M. (1992) Specificity of *Escherichia coli* endoribonuclease RNase E: *in vivo* and *in vitro* analysis of mutants in a bacteriophage T4 mRNA processing site. *Genes Dev* **6:** 149–159.

Engelberg-Kulka, H., Sat, B., Reches, M., Amitai, S., and Hazan, R. (2004) Bacterial programmed cell death systems as targets for antibiotics. *Trends Microbiol* **12:** 66–71.

Engelberg-Kulka, H., Amitai, S., Kolodkin-Gal, I., and Hazan, R. (2006) Bacterial programmed cell death and multicellular behavior in bacteria. *PLoS Genet* **2:** e135.

Fernandez De Henestrosa, A.R., Ogi, T., Aoyagi, S., Chafin, D., Hayes, J.J., Ohmori, H., and Woodgate, R. (2000) Identification of additional genes belonging to the LexA regulon in *Escherichia coli*. *Mol Microbiol* **35:** 1560–1572.

Galvani, C., Terry, J., and Ishiguro, E.E. (2001) Purification of the RelB and RelE proteins of *Escherichia coli*: RelE binds to RelB and to ribosomes. *J Bacteriol* **183:** 2700–2703.

Gerdes, K., Rasmussen, P.B., and Molin, S. (1986) Unique type of plasmid maintenance function: postsegregational killing of plasmid-free cells. *Proc Natl Acad Sci USA* **83:** 3116–3120.

Gerdes, K., Christensen, S.K., and Lobner-Olesen, A. (2005) Prokaryotic toxin-antitoxin stress response loci. *Nat Rev Microbiol* **3:** 371–382.

Golemis, E.A., and Brent, R. (1992) Fused protein domains inhibit DNA binding by LexA. *Mol Cell Biol* **12:** 3006–3014.

Halegoua, S., Hirashima, A., Sekizawa, J., and Inouye, M. (1976a) Protein synthesis in toluene-treated *Escherichia coli*. Exclusive synthesis of membrane proteins. *Eur J Biochem* **69:** 163–167.

Halegoua, S., Hirashima, A., and Inouye, M. (1976b) Puromycin-resistant biosynthesis of a specific outer-membrane lipoprotein of *Escherichia coli*. *J Bacteriol* **126:** 183–191.

Hayes, C.S., and Sauer, R.T. (2003) Cleavage of the A site mRNA codon during ribosome pausing provides a mechanism for translational quality control. *Mol Cell* **12:** 903–911.

Keren, I., Kaldalu, N., Spoering, A., Wang, Y., and Lewis, K. (2004) Persister cells and tolerance to antimicrobials. *FEMS Microbiol Lett* **230:** 13–18.

Korch, S.B., and Hill, T.M. (2006) Ectopic overexpression of wild-type and mutant *hipA* genes in *Escherichia coli*: effects on macromolecular synthesis and persister formation. *J Bacteriol* **188:** 3826–3836.

Lewis, L.K., Harlow, G.R., Gregg-Jolly, L.A., and Mount, D.W. (1994) Identification of high affinity binding sites for LexA which define new DNA damage-inducible genes in *Escherichia coli*. *J Mol Biol* **241:** 507–523.

McKenzie, G.J., Magner, D.B., Lee, P.L., and Rosenberg, S.M. (2003) The *dinB* operon and spontaneous mutation in *Escherichia coli*. *J Bacteriol* **185:** 3972–3977.

Masuda, Y., Miyakawa, K., Nishimura, Y., and Ohtsubo, E. (1993) *chpA* and *chpB*, *Escherichia coli* chromosomal homologs of the pem locus responsible for stable maintenance of plasmid R100. *J Bacteriol* **175:** 6850–6856.

Motiejunaite, R., Armalyte, J., Markuckas, A., and Suziedeliene, E. (2007) *Escherichia coli dinJ-yafQ* genes act as a toxin-antitoxin module. *FEMS Microbiol Lett* **268:** 112–119.

Munoz-Gomez, A.J., Santos-Sierra, S., Berzal-Herranz, A., Lemonnier, M., and Diaz-Orejas, R. (2004) Insights into the specificity of RNA cleavage by the *Escherichia coli* MazF toxin. *FEBS Lett* **567:** 316–320.

Neher, S.B., Villen, J., Oakes, E.C., Bakalarski, C.E., Sauer, R.T., Gygi, S.P., and Baker, T.A. (2006) Proteomic profiling of ClpXP substrates after DNA damage reveals extensive instability within SOS regulon. *Mol Cell* **22:** 193–204.

Opperman, T., Murli, S., Smith, B.T., and Walker, G.C. (1999) A model for a *umuDC*-dependent prokaryotic DNA damage checkpoint. *Proc Natl Acad Sci USA* **96:** 9218–9223.

Pedersen, K., Christensen, S.K., and Gerdes, K. (2002) Rapid induction and reversal of a bacteriostatic condition by controlled expression of toxins and antitoxins. *Mol Microbiol* **45:** 501–510.

Pedersen, K., Zavialov, A.V., Pavlov, M.Y., Elf, J., Gerdes, K., and Ehrenberg, M. (2003) The bacterial toxin RelE displays codon-specific cleavage of mRNAs in the ribosomal A site. *Cell* **112:** 131–140.

Redko, Y., Tock, M.R., Adams, C.J., Kaberdin, V.R., Grasby, J.A., and McDowall, K.J. (2003) Determination of the catalytic parameters of the N-terminal half of *Escherichia coli* ribonuclease E and the identification of critical functional groups in RNA substrates. *J Biol Chem* **278:** 44001–44008.

Sarmientos, P., Sylvester, J.E., Contente, S., and Cashel, M. (1983) Differential stringent control of the tandem *E. coli* ribosomal RNA promoters from the rrnA operon expressed in vivo in multicopy plasmids. *Cell* **32:** 1337–1346.

Shinagawa, H. (1996) SOS response as an adaptive response to DNA damage in prokaryotes. *EXS* **77:** 221–235.

Stenstrom, C.M., Jin, H., Major, L.L., Tate, W.P., and Isaksson, L.A. (2001) Codon bias at the 3′-side of the initiation codon is correlated with translation initiation efficiency in *Escherichia coli*. *Gene* **263:** 273–284.

Sunohara, T., Jojima, K., Tagami, H., Inada, T., and Aiba, H. (2004a) Ribosome stalling during translation elongation induces cleavage of mRNA being translated in *Escherichia coli*. *J Biol Chem* **279:** 15368–15375.

Sunohara, T., Jojima, K., Yamamoto, Y., Inada, T., and Aiba, H. (2004b) Nascent-peptide-mediated ribosome stalling at a stop codon induces mRNA cleavage resulting in nonstop mRNA that is recognized by tmRNA. *RNA* **10:** 378–386.

Tsilibaris, V., Maenhaut-Michel, G., Mine, N., and Van Melderen, L. (2007) What is the benefit to *Escherichia coli* of having multiple toxin-antitoxin systems in its genome? *J Bacteriol* **189:** 6101–6108.

Wade, J.T., Reppas, N.B., Church, G.M., and Struhl, K. (2005) Genomic analysis of LexA binding reveals the permissive nature of the *Escherichia coli* genome and identifies unconventional target sites. *Genes Dev* **19:** 2619–2630.

Wang, H.C., and Hickey, D.A. (2002) Evidence for strong selective constraint acting on the nucleotide composition of 16S ribosomal RNA genes. *Nucleic Acids Res* **30:** 2501–2507.

Zalucki, Y.M., Power, P.M., and Jennings, M.P. (2007) Selection for efficient translation initiation biases codon usage at second amino acid position in secretory proteins. *Nucleic Acids Res* **35:** 5748–5754.

Zhang, Y., Zhang, J., Hoeflich, K.P., Ikura, M., Qing, G., and Inouye, M. (2003) MazF cleaves cellular mRNAs specifically at ACA to block protein synthesis in *Escherichia coli*. *Mol Cell* **12:** 913–923.

Zhang, Y., Zhang, J., Hara, H., Kato, I., and Inouye, M. (2005a) Insights into the mRNA cleavage mechanism by MazF, an mRNA interferase. *J Biol Chem* **280:** 3143–3150.

Zhang, Y., Zhu, L., Zhang, J., and Inouye, M. (2005b) Characterization of ChpBK, an mRNA interferase from *Escherichia coli*. *J Biol Chem* **280:** 26080–26088.

Zhu, L., Zhang, Y., Teh, J.S., Zhang, J., Connell, N., Rubin, H., and Inouye, M. (2006) Characterization of mRNA interferases from *Mycobacterium tuberculosis*. *J Biol Chem* **281:** 18638–18643.

Supporting information

Additional supporting information may be found in the online version of this article.

Please note: Wiley-Blackwell are not responsible for the content or functionality of any supporting materials supplied by the authors. Any queries (other than missing material) should be directed to the corresponding author for the article.